

# COMPARISON OF CALCULATION METHODS FOR SMOKE AND HEAT EVACUATION FOR ENCLOSURE FIRES IN LARGE COMPARTMENTS

by

***Bart MERCI and Paul VANDEVELDE***

Original scientific paper

UDC: 656.085.5:628.83:519.876.5

BIBLID: 0354-9836, 11 (2007), 2, 181-196

*A comparative study is presented of different calculation methods with respect to the evacuation of smoke and heat in the case of enclosure fires in large compartments. These methods range from manual calculations, based on empirical formulae, over zone modeling to the use of computational fluid dynamics. The focus is on large single storey compartments. The differences between results obtained with the examined methods are discussed.*

Key words: *enclosure fires, smoke and heat evacuation, calculation methods, zone models, computational fluid dynamics*

## Introduction

At the stage of the design of smoke and heat evacuation systems (SHEVS), it is necessary to rely on a calculation procedure for a fire-safe solution. For single storey buildings, the calculation procedure NBN S21-208-1 is claimed to be valid. Some aspects are discussed below. There is also a European method CR12101-5. Again, some aspects are discussed below. For comparison reasons, we also consider some formulae reported in [1].

Using computer resources, it is possible to apply zone models, relying on the existence of a hot upper layer and a cold bottom layer. One of the basic assumptions in zone modeling is that there are no strong variations in *e. g.* temperature in horizontal directions. In this paper we will illustrate that this is not guaranteed for large compartments. We consider two zone model packages: OZONE [2] and CFAST [3].

The most detailed calculations are computational fluid dynamics (CFD) simulations, also known as “field models”. In this method, the compartment is sub-divided into many cells, constituting the computational “mesh”.

We apply all methods to two generic test cases. We do not consider the possibility of sprinklers, nor possible external influence factors (such as wind or snow).

## Features of the calculation methods

### Manual methods

A primary observation for the “manual” calculation methods considered here (NBN S21-208-1, CR 12101-5, and [1]) is that the procedure relies on “steady-state” assumptions. In particular, a “suitable” steady-state design fire source must be defined. This design fire is crucial for the entire outcome. The design fire is a fire for which the SHEVS must still operate appropriately. Implicitly it is assumed that smaller fires (in terms of area and/or heat release rate) will be dealt with appropriately by the SHEVS, too. (*e. g.* for the smoke rising in a high atrium, equipped for natural ventilation, it is not always guaranteed that the largest fire source is indeed the worst possible case), but this is beyond the scope of the present paper.

The required input data for the manual methods are:

- the design fire source, in terms of both heat release rate and dimensions (area and perimeter); this depends on the type of building,
- the smoke layer depth: the acceptable thickness of the hot upper smoke layer must be specified, and
- the compartment geometry: depending on the compartment dimensions and the configuration (*e. g.* ventilation from only one side), some model constants can be given a different value.

Given these input data, empirical formulae allow for the design of the SHEVS. It is important to note that, due to the empiricism, the manual methods are in principle only valid for the experimental configurations from which the empirical formulae have been constituted. In particular, it cannot be expected that the manual methods are suitable for complex geometries, but this is not the subject of the present paper.

Before going into more detail for the different methods, we also note that a general shortcoming of manual calculation methods is the neglect of heat transfer, both convective and radiative, from the hot smoke layer to the structure. In particular for large compartments, this may not be negligible. In zone models and CFD simulations, heat transfer normally is accounted for.

We now discuss the calculation procedure in some detail. We start with CR 12101-5. First the design fire is defined, in terms of area, perimeter, and heat release rate. The convective heat flux is then determined as:

$$Q_c = 0.8 Q_f = 0.8 q_f A_f \quad (1)$$

implying that 20% of the fire heat release rate is directly lost by radiation, *i. e.* is not transferred towards the hot smoke layer. Next, the smoke-free height  $Y$  is defined. If, the following empirical formula is applied for the mass flow rate at height  $Y$  in the smoke plume above the fire source:

$$M_f = C_e P \sqrt{Y^3}, \quad Y = 10 \sqrt{A_f} \quad (2)$$

For large compartments, such as considered here,  $C_e$  is assigned the empirical value 0.19. From expressions (1) and (2), the average hot smoke layer temperature rise, with respect to ambient temperature, due to the fire heat source, can be computed:

$$\theta_1 = \frac{Q_c}{cM_f} \quad (3)$$

where  $c = 1 \text{ kJ/kgK}$ , the value for air. If this temperature is acceptable, the volume flow rate, to be removed from the compartment, is computed as:

$$V = \frac{M_f T_1}{\rho_{\text{amb}} T_{\text{amb}}} \quad (4)$$

with  $T_1$  the absolute hot smoke layer temperature (in K):

$$T_1 = \theta_1 + T_{\text{amb}} \quad (5)$$

In case of natural ventilation, the total required free aerodynamic ventilation area is:

$$A_{v \text{ tot}} C_v = \frac{M_f T_1}{\sqrt{2\rho_{\text{amb}}^2 g d_1 \theta_1 T_{\text{amb}} \frac{M_f^2 T_1 T_{\text{amb}}}{(A_i C_i)^2}}} \quad (6)$$

The loss coefficients are usually assigned the value 0.6. If  $A_i C_i$  is large compared to each ventilation area  $A_{v n}$ , the following relation is valid for the mass flow rate through ventilator  $n$ :

$$M_n = \frac{\rho_{\text{amb}} A_{v n} C_{v n} \sqrt{2g d_1 \theta_1 T_{\text{amb}}}}{T_1} \quad (7)$$

The design must be such that  $\sum_n M_n = M_f$

In case of mechanical ventilation, the number of extraction points becomes important in order to avoid “plug-holing”. This is the phenomenon that the smoke layer under a ventilator is not sufficiently thick, so that air is removed through the ventilator, rather than pure smoke. The required number of extraction points is determined from the critical extraction rate. For a ventilator close to the wall, this is:

$$M_{\text{crit}} = 1.3 \sqrt{g d_1^5 T_{\text{amb}} \frac{\theta_1}{T_1^2}} \quad (8)$$

For a ventilator that is further away from the wall than its own characteristic width  $D_v$ , the expression becomes:

$$M_{\text{crit}} = \frac{2.05 \rho_{\text{amb}} \sqrt{g T_{\text{amb}} \theta_1} d_1^2 \sqrt{D_v}}{T_1} \quad (9)$$

The required number of extraction points is  $N \geq M_f/M_{\text{crit}}$ .

In NBN S21-208-1, the philosophy is very similar to CR12101-5, but there are some differences in implementation. First of all, the design fire is primarily determined by its dimension. According to the application category, the fire source can vary from 3 m (category 1) to 9 m (category 4). The fire heat release rate per unit area is then specified as:

$$\text{– for natural ventilation: } q_f = 250 \text{ kW/m}^2, \text{ and} \quad (10)$$

$$\text{– for mechanical ventilation: } q_f = 500 \text{ kW/m}^2. \quad (11)$$

In fact, there is no strong scientific support for these values. But, in contrast to CR12101-5, where quite some freedom is allowed in the design fire specification, expressions (10) and (11) have the advantage of simplicity: once the dimensions of the fire source have been specified, the fire source is completely defined. In NBN S21-208-1, the following expression is applied for the mass flow rate:

$$M_f = 0.188 P \sqrt{Y^3} \quad (12)$$

This is the same as expression (2). Expression (1) is again used for the convective heat release rate, in the absence of sprinklers. If there are sprinklers, the factor 0.8 is reduced to 0.5. Expressions (3) and (4) are also used in NBN S21-208-1. In the case of natural ventilation, a slightly different formula than (6) is used:

$$A_v C_v = \frac{M_f}{\rho_{\text{amb}}} \sqrt{\frac{T_1^2 \frac{A_v C_v}{A_i C_i} T_{\text{amb}} T_1}{2 g d_1 \theta_1 T_{\text{amb}}}} \quad (13)$$

When  $A_i C_i$  is much larger than  $A_v C_v$ , expression (7) is recovered. A critical area value is specified for natural ventilation in NBN S21-208-1, in order to avoid plug-holing:

$$A_v C_v < (A_v C_v)_{\text{crit}} = 1.4 d_1^2 \quad (14)$$

There must also be at least one extraction point per 400 m<sup>2</sup>. In the case of mechanical ventilation, the expression for the critical flow rate in NBN S21-208-1 is:

$$V_{\text{crit}} = \frac{2}{T_1} \sqrt{g d_1^5 (T_1 - T_{\text{amb}}) T_{\text{amb}}} \quad (15)$$

Note that a critical volume flow rate is specified, rather than a mass flow rate (8).

In [1], the formula for the mass flow rate is different:

$$M_f = 0.071 \sqrt[3]{Q_c (Z - z_o)^5} [1 - 0.026 \sqrt[3]{Q_c^2 (Z - z_o)^5}] \quad (16)$$

where  $Z$  is the height above the fire source and  $z_o$  is the fire source virtual origin height:

$$z_o = 0.083 \sqrt[3]{Q_f^2} - 1.02D \quad (17)$$

with  $D$  the fire source (hydraulic) diameter. Note that in formula (16) both the geometry and the heat release rate of the fire determine the mass flow rate. Expressions (3) and (4) are again applied. In case of natural ventilation, the extraction area is determined as:

$$A_v C_v = \frac{M_f}{\rho_0} \sqrt{\frac{T_1 \frac{A_v^2}{A_i} T_{amb}}{2gd_1 (T_1 - T_{amb}) \frac{T_{amb}}{T_1}}} \quad (18)$$

which is, under the assumption that  $C_i = C_v$ , identical to expression (13). In case of mechanical ventilation, the expression for the critical volume flow rate in [1] is:

$$V_{crit} = 0.00887 \beta \sqrt{d_1^5 [(T_1 - T_{amb}) T_{amb}]} \quad (19)$$

to be compared to expressions (9) and (15). Beta is equal to 2 (close to walls) or 2.8 (away from walls).

It is interesting to discuss the differences between expression (9), (15) and (19). Since, in a first approximation, a ventilator has a constant volume flow rate, rather than a constant mass flow rate, it seems more natural to consider a critical volume flow rate, rather than a critical mass flow rate. In this sense, expressions (15) and (20) are the most logical. But, in expression (9), the smoke density in the ventilator is accounted for through the appearance of  $T_1$  in the denominator of the right hand side, so that (9) actually defines a critical volume flow rate. In (15) the  $T_1$  is still present in the denominator, but its origin is not clear, since there is a volume flow rate at the left hand side. Consequently, the number of extraction points, computed from (15) (and thus in NBN S21-208-1), will always be higher than what is computed from (9) (CR12101-5), since the temperature of the smoke layer is higher than ambient temperature.

### Zone modeling

In zone modeling, a basic assumption is the existence of two separated “layers”: a hot upper layer and a cold bottom layer. The interface between these two layers is horizontal and in each of the two zones, spatial uniformity is assumed for all properties at every time instant. This is often a very stringent assumption, limiting the range of applicability of zone models considerably. In particular, zone models have not been developed

for the conditions in the examples of the present paper: in large compartments, there are variations in horizontal planes. Moreover, during the early stages, a very thin upper layer is assumed under the entire ceiling in zone models, which is not in line with reality. One of the purposes of the present paper is to examine to what extent the zone model approach remains valid under rather extreme circumstances.

The volume of the plume is typically small, compared to the smoke layer, and is thus typically neglected. Further, it is assumed that possible mixing through the interface can be neglected, compared to entrainment of gases into the plume. The fire source is seen as an enthalpy source. The plume is a kind of “pump” for mass and enthalpy from the cold bottom layer towards the hot upper layer.

A large difference compared to CFD is that the conservation of total momentum is not explicitly imposed. Consequently, it becomes impossible to accurately predict transport times over large distances (*e. g.* smoke rise in an atrium).

Heat transfer towards the structure is typically accounted for.

It is important to appreciate that, in zone model simulations, there are sub-models for:

- fire source heat release rate (which is normally specified),
- entrainment of air into the plume,
- heat transfer (conduction, convection and radiation), and
- possibly combustion (incomplete combustion).

We consider two zone model packages: OZONE and CFAST. Details of these packages are found in their manuals. Important to remark is that CFAST contains McCaffrey’s entrainment model [4], which accounts for differences in entrainment behavior in the flame region, the plume zone and the intermittent region in between. This entrainment model is applicable for a wide range of fire sources and ceiling heights. In OZONE the choice can be made between 4 entrainment models (among which McCaffrey’s model), but care must be taken that an appropriate choice is made, valid for the test case under study.

### *CFD simulations*

As already mentioned, in CFD simulations the compartment is sub-divided into many computational cells (the “mesh”). For each individual cell, the basic physical conservation laws are expressed: conservation of mass, total momentum, and energy. Furthermore, combustion is to be accounted for in the case of fire, so that additional transport equations must be solved.

Without going into detail, it is important to appreciate that CFD simulations still contain many sub-models:

- turbulence: with present available computer resources, it is impossible to make direct numerical simulations of turbulent flows of practical interest (*i. e.* with high Reynolds numbers and/or in complex geometries), because of the large range of time and length scales in the turbulent eddies,

- chemistry: similarly it is impossible to account for detailed reaction mechanisms with finite rate kinetics, because then the turbulent reacting flow simulations become computationally intractable,
- heat transfer: models are applied for both convective and radiative heat transfer, and
- interactions: there is interaction between the different phenomena, which must also be accounted for and must be modeled.

In principle, flame spread can be simulated and coupled to CFD for the surrounding reacting flow field. In practice, this is again computationally expensive and scientifically in the development phase. So it is common practice to prescribe the fire source in CFD simulations of fire.

In the present paper, we use the package Fire Dynamics Simulator (FDS), developed at NIST [5]. This should not create the impression that we believe that this package would be superior, compared to other existing CFD simulation packages for fire. Neither do we claim the opposite. Rather, the applications in this paper must be seen as illustrations of the possibilities of the three major classes of calculation methods, as described above.

To conclude this section, we remark that it is important to perform a grid sensitivity study when CFD simulation results are used for the design of SHEVS. The coarseness of the mesh is usually determined by the computer power at hand, so that it may be tempting to present the obtained results as “reliable”. Only a grid sensitivity study can yield an indication as to what extent this is the case.

## Test cases

### *Supermarket*

The first example is a simplified supermarket of width 35 m, length 70 m, and height 4 m. There are 6 doors of 7 m wide and 2 m high. This geometry, including 8 extraction points, is shown in fig. 1.

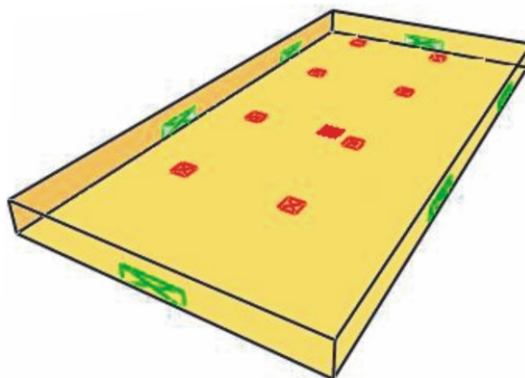


**Figure 1.** Simplified supermarket with 8 extraction points (color image see on our web site)

We consider mechanical ventilation.

The design fire is defined as a square of  $3 \times 3$  m with total heat release rate  $Q_f = 4500$  kW. This is possible for both CR12101-5 and NBN S21-208-1 (category 1). The smoke-free height for the manual calculation methods is defined as  $Y = 3$  m. We now first use the manual methods to design the SHEVS and then apply the other methods to make some a posteriori observations.

Calculation method CR12101-5 yields  $M_f = 11.8$  kg/s from expression (2) and  $\theta_1 = 304$  °C from expression (3). This value is too high (*e. g.* [1, 6, 7]). Choosing *e. g.*  $\theta_1 = 150$  °C as a reasonable value – note that this is a personal choice – expression (3) yields  $M_f = 24$  kg/s. Note that, from expression (2), one can compute that this corresponds to  $Y = 4.8$  m, which is impossible since the ceiling height is only 4 m. This indicates that a stable steady situation is unlikely. Expression (4) then gives the volume flow rate:  $V = 30.2$  m<sup>3</sup>/s, with  $p_{amb} = 101300$  Pa and  $T_{amb} = 293$  K. Under the assumption that a typical ventilator dimension is  $D_v = 1$  m and that the ventilators are sufficiently far from the walls (see fig. 1), expression (9) gives the critical mass flow rate:  $M_{crit} = 3.65$  kg/s. This shows that, according to CR12101-5, 7 ventilators are required.

The same calculations can be done for NBN S21-208-1. The only difference is expression (15) for the critical flow rate:  $V_{crit} = 3.0$  m<sup>3</sup>/s. This shows that, according to NBN S21-208-1, 10 ventilators are required. As already mentioned, this is a higher value than obtained with CR12101-5.

Still imposing the hot layer temperature rise  $\theta_1 = 150$  °C, the formulae of [1] yield the same results. The critical volume rate now becomes  $V_{crit} = 5.2$  m<sup>3</sup>/s, so that 6 ventilators are required.

We now discuss zone model results. We define openings in the ceiling so that the mass flow rate  $M_f = 24$  kg/s is extracted. Since it is not feasible to define mechanical extraction, we define openings in the ceiling with total area determined from expression (6), with  $d_1 = 1$  m and  $C_v = 0.4$  (which is the value used in OZONE), yielding  $A_v = 27$  m<sup>2</sup>. Using McCaffrey's entrainment model [1], fig. 2 shows the evolution of the upper layer temperature and the interface height between the hot upper layer and the cold bottom layer. The upper two figures show results obtained with OZONE, the bottom two figures are CFAST results. We see large differences between the results. We note that, with respect to temperature, the steady-state value is not yet reached with OZONE after 20 minutes, while the end temperature is practically reached after about 10 minutes with CFAST. We also notice that the temperatures are higher with CFAST than with OZONE. This is due to the high convection coefficient in OZONE (25 W/m<sup>2</sup>K), so that much heat is transferred from the hot smoke layer towards the structure. With respect to the interface height, the situation becomes steady after 10 minutes. Note that the smoke-free height is about 1.8 m with OZONE, which is substantially less high than the starting point in the manual calculations ( $Y = 3$  m), while it is about 3.4 m with CFAST. This is due to the lower loss coefficient value in OZONE ( $C_v = 0.4$ ) than in CFAST ( $C_v = 0.6$ ), so that smoke emerges from the compartment more easily in CFAST. We recall once again that the mechanical extraction has been replaced by ceiling openings in the zone model calculations, as described above. The major conclusion to be drawn from the comparison of the



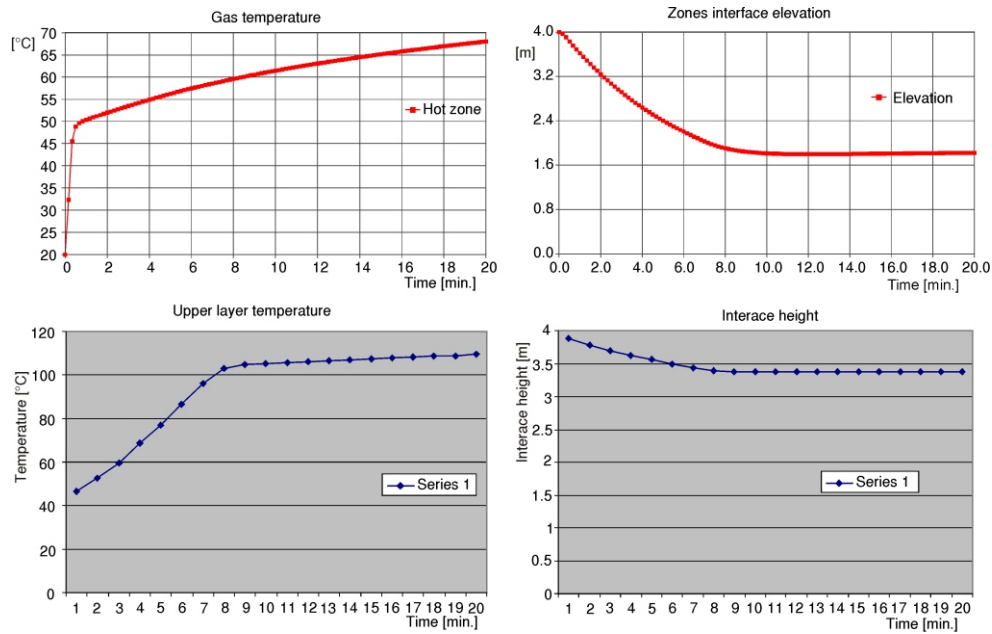


**Figure 2. Evolution of hot layer temperature and interface height with zone models. Top figures: OZONE; bottom figures: CFAST**

zone model results is that, dependent on the sub-model choices and model parameter values, strongly different results can be obtained for one and the same configuration.

To conclude the first example, we now discuss CFD simulation results. There are 8 extraction points (mechanical ventilation again) and the extraction flow rate is fixed at  $30 \text{ m}^3/\text{s}$ . The basic computational mesh consists of  $140 \times 70 \times 8 = 78400$  cubic cells (so that each cell dimension is 0.5 m). A mesh refinement study has been performed by comparison to results on a mesh of  $280 \times 140 \times 16 = 627200$  cells (with dimension 0.25 m per cell).

Figure 3 shows temperature contours after 20 minutes in vertical planes. Note that there are variations of temperature in horizontal planes, in particular close to the ceiling. This means that one of the basic assumptions for zone modeling to be valid, is not fulfilled. Note also that the same assumption is implicitly present in the manual calculation methods, since the entire smoke layer is assumed to be at uniform temperature.

We remark that it is not really possible to define a smoke-free height in the CFD simulations, because there are places where the smoke almost reaches the floor (not shown). In manual calculations or zone model results, this cannot be seen because only mean values are available.

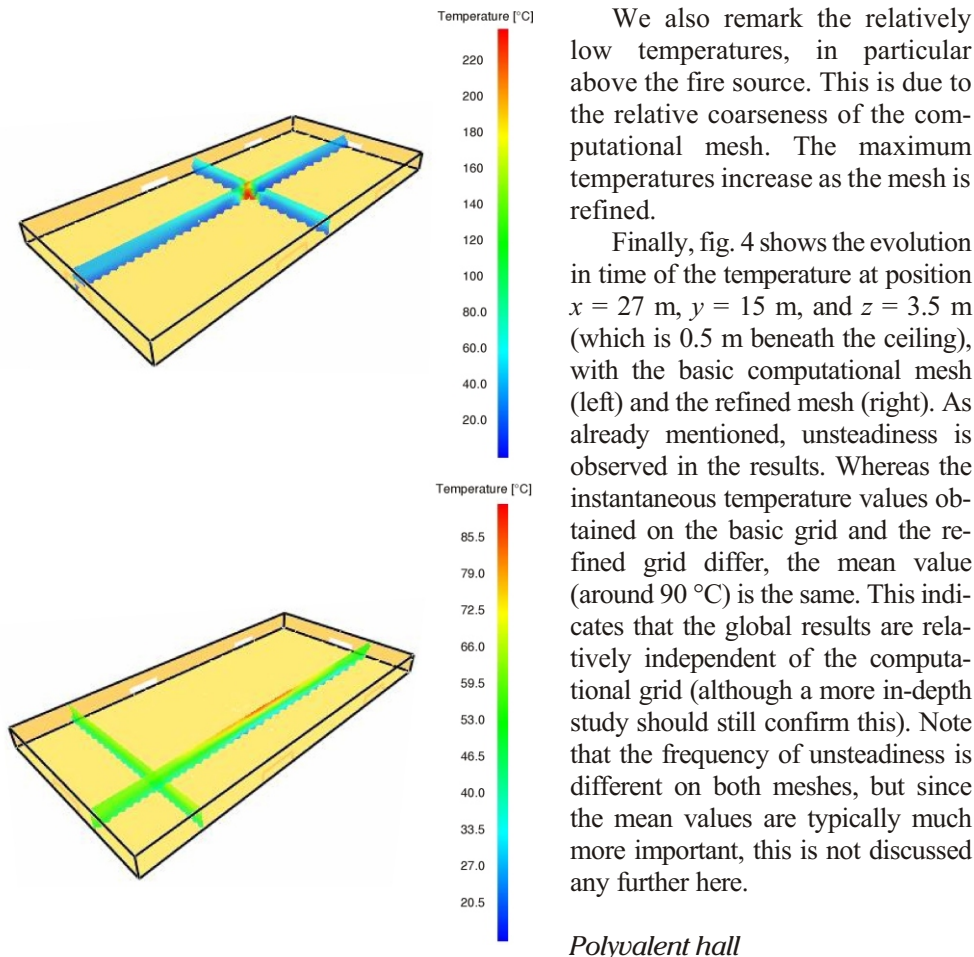


**Figure 3. Temperature after 20 minutes in vertical planes (CFD results) (color image see on our web site)**

The width is 66 m, the length is 95 m, and the height is 11 m. There are 10 gates of 5.2 m wide and 2.1 m high. These are positioned as follows: two times 4 gates along the long sides of the building and two gates at one of the short ends.

We consider natural ventilation. The fire source is taken as  $9 \times 9$  m with total heat release rate equal to  $\dot{Q}_f = 20250$  kW. As in the previous example we use the manual methods to design the SHEVS and then apply the other methods a posteriori.

Method CR12101-5 yields  $M_f = 35.5$  kg/s and  $\theta_1 = 456$  °C. This value is again too high and we choose  $\theta_1 = 150$  °C, leading to  $M_f = 108$  kg/s. This corresponds to  $Y = 6.3$  m, according to expression (2), which is plausible, since the smoke layer thickness is then 4.7 m.

We also remark the relatively low temperatures, in particular above the fire source. This is due to the relative coarseness of the computational mesh. The maximum temperatures increase as the mesh is refined.

Finally, fig. 4 shows the evolution in time of the temperature at position  $x = 27$  m,  $y = 15$  m, and  $z = 3.5$  m (which is 0.5 m beneath the ceiling), with the basic computational mesh (left) and the refined mesh (right). As already mentioned, unsteadiness is observed in the results. Whereas the instantaneous temperature values obtained on the basic grid and the refined grid differ, the mean value (around 90 °C) is the same. This indicates that the global results are relatively independent of the computational grid (although a more in-depth study should still confirm this). Note that the frequency of unsteadiness is different on both meshes, but since the mean values are typically much more important, this is not discussed any further here.

#### *Polyvalent hall*

The second example concerns a polyvalent hall for e. g. sports manifestations, mass events, exhibitions.

The geometry is depicted in fig. 5.

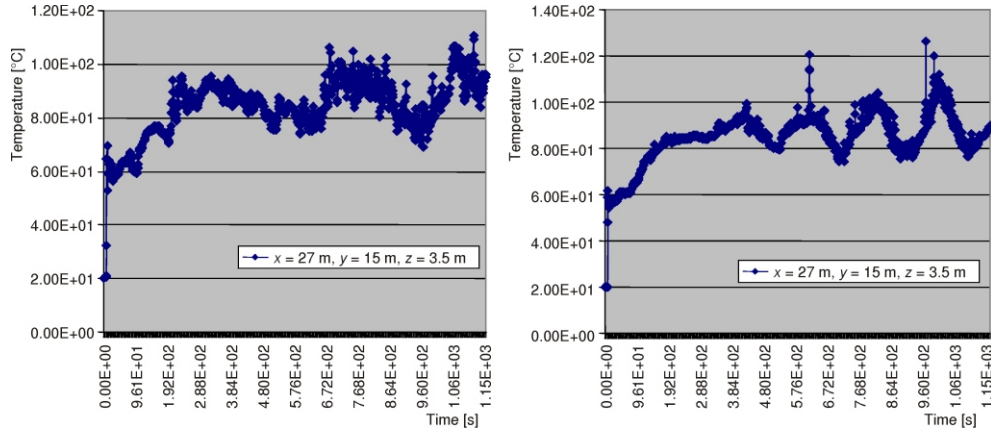


Figure 4. Temperature evolution at a certain point with the basic computational grid (left) and with a refined grid (right)

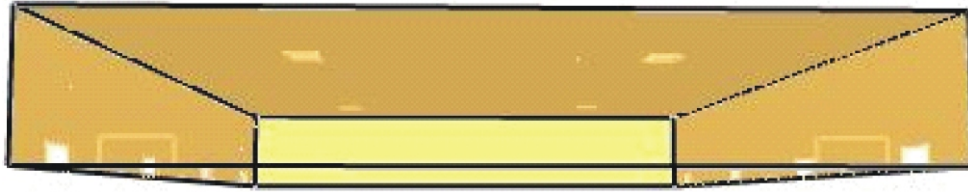
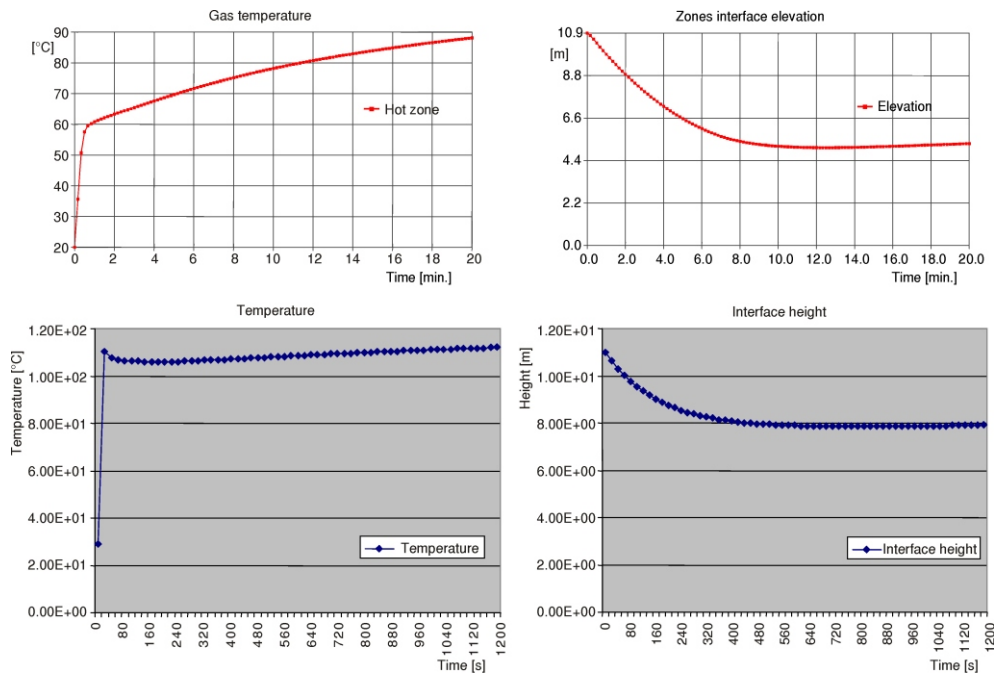


Figure 5. Geometry of the polyvalent hall

The volume flow rate is:  $V = 130 \text{ m}^3/\text{s}$ , again with  $p_{\text{amb}} = 101300 \text{ Pa}$  and  $T_{\text{amb}} = 293 \text{ K}$ . The inlet area for fresh air is  $A_i = 10 \cdot 5.2 \cdot 2.1 = 109.2 \text{ m}^2$ . Thus, with  $C_i = 0.4$ , the required ventilation area for the smoke is obtained from expression (6):  $A_{v \text{ tot}} C_v = 21.3 \text{ m}^2$ . With  $C_v = 0.4$ , this shows that, according to CR12101-5, an area  $A_{v \text{ tot}} = 53 \text{ m}^2$  is required.

With NBN S21-208-1 the calculations are completely similar again. Expression (13) yields, after some iterations,  $A_{v \text{ tot}} C_v = 21.3 \text{ m}^2$  or  $A_{v \text{ tot}} = 53 \text{ m}^2$  (with  $C_v = 0.4$ ). This result is identical to the result with CR12101-5.

Using the same values  $\theta_1 = 150 \text{ }^\circ\text{C}$  and thus  $M_f = 108 \text{ kg/s}$ , expression (16) yields  $Z - z_0 = 9.7 \text{ m}$ . Using the hydraulic diameter value  $D_f = 9 \text{ m}$ , expression (17) yields  $z_0 = -4.8 \text{ m}$ , so that  $Y = 4.9 \text{ m}$  and the smoke layer thickness is  $6.1 \text{ m}$ . The accuracy of expression (16) can be questioned: it relies on a fire point source, while the area is rather large here. Expression (18) provides, after some iterations,  $A_{v \text{ tot}} C_v = 18.4 \text{ m}^2$ , or  $A_{v \text{ tot}} = 46 \text{ m}^2$  (again  $C_v = 0.4$ ), which is lower than the previous value.



**Figure 6. Evolution of hot layer temperature and interface height with zone models. Top figures: OZONE; bottom figures: CFAST**

From now on we consider a configuration of 4 openings in the ceiling of  $3 \times 4$  m each. This gives a total area  $A_{v\text{ tot}} = 48 \text{ m}^2$ . Figure 6 shows the results with the two zone models. Again the top figures are obtained with OZONE and the bottom figures with CFAST. In OZONE, McCaffrey's entrainment model is applied. With OZONE we observe that the interface height corresponds quite well with the value obtained from the expressions of [1], although we recall that there is no direct correspondence between the interface height in the zone models and the bottom of the hot upper layer. As in fig. 2, we see that the steady-state temperature has not been reached yet with OZONE after 20 minutes. All other observations are in line with the previous example (fig. 2), too: CFAST reaches steady-state much earlier; temperatures in CFAST are higher than in OZONE (due to differences in convection coefficient); the interface height is higher in CFAST than in OZONE ( $C_v = 0.6$  vs.  $C_v = 0.4$ ).

We now examine CFD simulation results. We use cubic cells with dimension 1 m. This implies  $66 \times 95 \times 11 = 68970$  cells. It is not 100% guaranteed that this is sufficiently fine to capture all phenomena, but for the purpose of the present paper, we did not perform a grid refinement and rely on the CFD results with respect to the global observations.

Figure 7 shows the visibility in vertical planes after 20 minutes. The effect of asymmetry (recall that there are two gates at only one of the short ends) is small. We ob-

serve that the smoke layer thickness is the largest in the neighborhood of the fire source. The average smoke layer thickness is about  $d_1 = 7.9$  m. Clearly there is variation of the smoke layer thickness in space (which cannot be seen in manual methods and zone models), so that at the worst positions, *e. g.* in the corners, the smoke layer is clearly thicker.

In order to illustrate the possibilities of CFD in SHEVS design, we now examine a configuration where there are 28 openings in the ceiling of 2 × 1 m each. Figure 8 clearly illustrates a substantial improvement in visibility, compared to fig. 7. The average smoke layer thickness is now  $d_1 = 6.8$  m.

We conclude the discussion of this example by comparing the different calculation methods. The results are summarized in tab. 1. For the CFD simulations, the smoke-free height has been determined as an average value. For the zone models, the interface height is used to determine the smoke-free height. We see

that the CFD results are the most pessimistic and thus, from a safety point of view, the most conservative. We also see that the formulae from [1] are closest to the CFD results. The smoke-free height determined with CR12101-5 and NBN S21-208-1 is identical. With OZONE, a smoke-free height is obtained that is in line with the CFD results for 28 openings. Recall that McCaffrey's entrainment model was used. The zone model CFAST clearly predicts by far the largest smoke-free height, so that this model cannot be judged as conservative for the test cases examined. Recall that the zone models are applied here

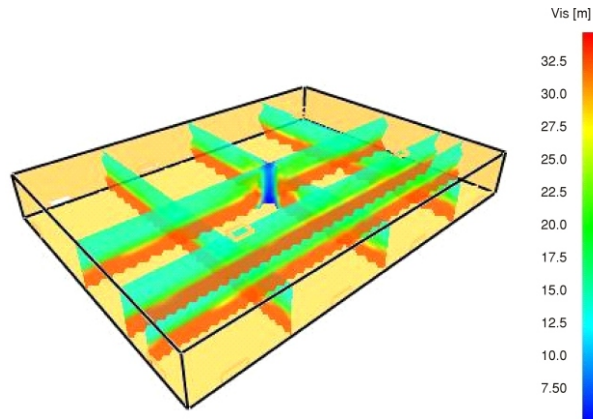


**Figure 7. Visibility after 20 minutes in vertical planes (CFD results) (color image see on our web site)**

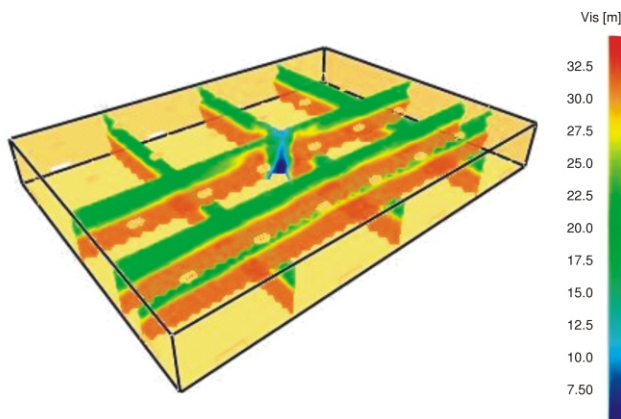


**Figure 8. Visibility after 20 minutes in vertical planes (CFD results); 28 openings (color image see on our web site)**

in conditions for which they were not developed, since the basic assumption of uniformity in horizontal planes is not fulfilled. In the large compartment, a very thin upper layer is presumed under the entire ceiling during the early stages, which does not correspond to the physical situation.

**Table 1. Smoke-free height with the different calculation methods**

	CR12101-5	NBN S21-208-1	[1]	OZONE	CFAST	CFD (4)	CFD (28)
<i>Y</i>	6.3 m	6.3 m	4.9 m	5.2 m	8.0 m	4.1 m	5.2 m

## Conclusions

Different classes of calculation methods have been applied to two example test cases of large single storey compartments.

The manual methods CR12101-5 and NBN S21-208-1 are very similar in philosophy and contain almost identical formulae. It was pointed out that NBN S21-208-1 is more conservative with respect to the critical volume flow rate through ventilators, although it is not certain that the more conservative formula is based on scientific arguments. The formulae of [1] are somewhat different. In particular, both the geometry and the heat release rate of the design fire are accounted for in the determination of the smoke mass flow rate at a certain height. A common draw-back of the manual methods is the fact that they are steady, while during the early stages of a fire, when people must be evacuated or an intervention can take place, the situation can be completely different from the steady-state situation (with the design fire). Moreover, convective and radiative heat transfer from the smoke layer towards the structure is typically neglected.

Large differences have been observed between the two zone models, OZONE and CFAST. With OZONE, lower temperatures and a slow evolution towards steady-state are observed, due to a relatively high convection coefficient (due to which the smoke transfers much heat towards the structure). The interface height, on the other hand, is lower than with CFAST, due to a lower loss coefficient. With respect hereto, OZONE can thus be considered as more conservative than CFAST. We recall that the entrainment model is important in zone models and that McCaffrey's model, accounting for differences in entrainment in the flame region and the plume region, seems appropriate under many circumstances.

Some possibilities of CFD simulations have been illustrated by means of FDS results. The importance of a grid refinement study has been highlighted. Unsteadiness can be seen in CFD results. Moreover, the effect of different configurations on local temperature or visibility can readily be examined. Also, the evolution during early stages of a fire, which are relevant with respect to evacuation or possible intervention, can be studied with CFD. It is clear that much more information can be gained from CFD simulations



than with the manual methods or the zone models, but, of course, the price to pay is that CFD calculations are much more time consuming and require more skills from the use for correct application.

## Nomenclature

$A_f$	– fire source area, [m <sup>2</sup> ]
$A_i$	– air inlet area, [m <sup>2</sup> ]
$A_{v\ tot}$	– total ventilation area, [m <sup>2</sup> ]
$C_e$	– model constant, [–]
$C_i$	– loss coefficient for air inlet opening, [–]
$C_v$	– loss coefficient for ventilation opening, [–]
$c$	– specific heat capacity, [kJkg <sup>-1</sup> K <sup>-1</sup> ]
$D$	– fire source (hydraulic) diameter, [m]
$D_v$	– characteristic ventilator width, [m]
$d_l$	– smoke layer thickness, [m]
$g$	– gravity constant (= 9.81 ms <sup>-2</sup> )
$M_{crit}$	– critical mass flow rate, [kgs <sup>-1</sup> ]
$M_f$	– smoke mass flow rate, [kgs <sup>-1</sup> ]
$P$	– fire source perimeter, [m]
$Q_c$	– convective heat release rate, [kW]
$Q_f$	– fire heat release rate, [kW]
$q_f$	– fire heat release rate per unit area, [kWm <sup>-2</sup> ]
$T_{amb}$	– absolute ambient temperature, [K]
$T_l$	– hot layer absolute temperature, [K]
$V$	– volume flow rate, [m <sup>3</sup> s <sup>-1</sup> ]
$x, y, z$	– Descartes coordinates
$Y$	– smoke-free height, [m]
$Z$	– height above the fire source, [m]
$z_o$	– virtual origin height, [m]

## Greek letters

$\beta$	– constant
$\rho$	– density, [kgm <sup>-3</sup> ]
$\theta_l$	– hot layer temperature rise, [K or °C]

## References

- [1] Klote, J. H., Milke, J. A., Principles of Smoke Management, Society of Fire Protection Engineers, 2002
- [2] Franssen, J.-M., OZONE v2.0, University, Liège, Belgium
- [3] <http://fast.nist.gov/>
- [4] McCaffrey, B. J., Momentum Implications for Buoyant Diffusion Flames, *Combustion and Flame*, 52 (1983), 2, pp. 149-167
- [5] <http://fire.nist.gov/fds>

Authors' addresses:

*B. Merci*<sup>(1, 2)</sup>, *P. Vandevelde*<sup>(1, 3)</sup>

- <sup>(1)</sup> Ghent University – UGent, Faculty of Engineering, Department of Flow, Heat and Combustion Mechanics  
41, Sint-Pietersnieuwstraat, B-9000 Ghent, Belgium
- <sup>(2)</sup> Postdoctoral fellow of the Fund of Scientific Research, Flanders, Belgium (F.W.O.-Vlaanderen)  
5, Egmontstraat, B-1000 Brussels, Belgium
- <sup>(3)</sup> WFRGENT NV, 711, Ottergemsesteenweg, B-9000 Ghent, Belgium

Corresponding author B. Merci  
E-mail: bart.merci@UGent.be

Paper submitted: March 30, 2006  
Paper revised: July 30, 2006  
Paper accepted: September 1, 2006